American Journal of Optics and Photonics
2014; 2(4): 54-64
Published online October 30, 2014 (http://www.sciencepublishinggroup.com/j/ajop)
doi: 10.11648/j.ajop.20140204.12
ISSN: 2330-8486 (Print); ISSN: 2330-8494 (Online)

Influence of orbital hybridization on Kerr nonlinearity of a heavy metal borate glass: Scaling of polarizability and the imaginary contribution of optical susceptibility

Fouad El-Diasty[1, *], Fathy A. Abdel-Wahab[1], Manal Abdel-Baki[2], Fouad A. Moustafa[2]

[1]Physics Department, Faculty of Science, Ain Shams University, Abbasia, 11566 Cairo, Egypt
[2]Glass Department, National Research Centre, Dokki 12311 Giza, Egypt

Email address:
fdiasty@yahoo.com (F. El-Diasty)

To cite this article:
Fouad El-Diasty, Fathy A. Abdel-Wahab, Manal Abdel-Baki, Fouad A. Moustafa. Influence of Orbital Hybridization on Kerr Nonlinearity of a Heavy Metal Borate Glass: Scaling of Polarizability and the Imaginary Contribution of Optical Susceptibility. *American Journal of Optics and Photonics.* Vol. 2, No. 4, 2014, pp. 54-64. doi: 10.11648/j.ajop.20140204.12

Abstract: Photonics properties of glasses can be designed by controlling their complex Kerr nonlinearity. Chemical structure and bonding properties are considered as the origin of glass third-order susceptibilities. Investigation of the role of orbital hybridization on the glass electronic polarizability and third-order susceptibility is carried out. Thus, series of heavy metal lead borate glass of the composition $0.25B_2O_3$–$0.75PbO$ is prepared by melt quenching technique. Orbital hybridization, as a linear combination for valence electron wave functions of *p*- and *d*-block elements, is obtained through structural co-substitution of very small contents of Cr_2O_3 and/or SeO_2, by B_2O_3. It get succeed to tune the glass nonlinear optical characteristics such as; the complex components of third-order susceptibility. Scaling roles describing the relations between oxide ion polarizability and index of refraction and between imaginary part of third-order susceptibility and band gap energy are proposed. The glasses exhibit zero-dispersion wavelength at 1.55 μm band which is needed for telecommunication devices. The polarizability approach is applied to analyze and explain the obtained glass properties.

Keywords: Glass, Susceptibility, Polarizability, Orbital Hybridization

1. Introduction

Metal oxides display properties such as piezoelectricity, superconductivity, negative thermal expansion, ionic conductivity, high-temperature superconductor and transparent conductors. Transition metal oxides are fundamental ingredients for the smart and functional glasses. Ruby (Cr: Al_2O_3) and Nd:YAG ($Y_3Al_5O_{12}$) lasers, the well-developed nonlinear optical crystals $LiNbO_3$ and $Ba_2NaNb_5O_{15}$, are advanced examples for metal oxides glass photonic applications.

Chromium, as paramagnetic transition ion has various oxidation states; Cr^{3+}, Cr^{4+}, Cr^{5+} and Cr^{6+}, where Cr^{4+} [1] and Cr^{6+} [2], is considered as most stable ions. Chromium with $3d^2$ configurations is of interest in solid state laser due to its ability to generate laser emission in the near infrared spectral region between 1.2 and 1.7 μm. For instance, Cr^{4+}-doped forsterite (Mg_2SiO_4) emits from 1.167 to 1.345 μm [3].

In optical telecommunication systems, chalcogenide elements are used due to their less multiphonon relaxation [4, 5] and semiconductor-like property [6, 7]. They are also used in all-optical processes including switching, wavelength conversion, amplification, lasing, pulse compression, and slow light [8, 9]. A selenide based-glass can be doped with fluorescent rare-earth ions (emit at wavelength around 1 μm) which is stable against crystallization during fiberization [10]. In selenium, the 4*p*-electrons occupy two bonding orbitals representing covalent bonding and one orbital named a lone-pair.

Borate glasses are composed of microdomains of boroxol rings [11]. Near glass-transition temperature, they are broken up leading to a more open structure which offers excellent host material to incorporate trivalent rare earth ions. Great progress has been made in the field of nonlinear optical (NLO) materials since the advent of the first "high-tech" borate material β-BaB_2O_4 because of their high UV transmittance [12] combined with a high damage threshold.

Due to its higher polarizability and lower melting

temperatures [13], existing of Pb ions in glass network provides high refractive index and shifts the UV-electronic edge noticeably towards IR region of spectrum. Many heavy metal glasses, due to their low phonon energies and small field strength of their element ingredients, can be used as gain media for upconversion lasers [14, 15]. The difference between atomic masses of lead and boron increases the thermal stability and decreases the phonon energy of the glass which are needed for many spectroscopic applications.

Mixed valence effect [16] in glass is needed for photonic-crystals [17], for strong optical field confinement (which allows small waveguide bend radii) [18-20] and for controlled nonlinearity [21]. Development of new heavy-metal oxide glasses [22] with high optical nonlinearity is an important issue for harmonic generation, fiber telecommunication, ultrafast optical switches, power limiters, real-time holography, self-focusing, white-light continuum generation, and many other photonic applications.

As shown above, the effect of 3*d*-4*p* orbital hybridization of Cr_2O_3 and SeO_2 on the electronic structure and two-photon absorption of heavy metal borate glass was studied [23]. In the present work we continue studying the effect of orbital hybridization on the dispersion of nonlinear optical properties of heavy metal borate glasses. Phenomenological relation between the maximum values of imaginary part of third-order susceptibility with band gap energy is proposed. The obtained results may help to understand more the suitability of the studied glass in a diversity of photonic applications. Chemical bond approach is used to explain the obtained hyperpolarizability of the prepared glass.

2. Experimental

2.1. Glass Preparation

Table 1. *Glass compositions, Abbe dispersion number (V_d), static refractive index (n_0), dispersion energy (E_d), oscillation energy (E_o), lattice energy (E_l), direct optical energy gap (E_g) and wavelength for zero dispersion (λ_c)*

	No.	Glass compositions	V_d	n_o	E_d(eV)	E_o (eV)	E_l(eV)	E_g (eV) [23]	λ_{zero}(μm)
	1	0.25B2O3-0.75PbO (base)	43.91	1.5885	9.20	6.04	0.19	3.37	1.6633
	2	0.002SeO2-0.248B2O3-0.75PbO	57.59	1.7702	15.0	7.03	0.21	2.42	1.6320
1st series	3	0.004 SeO2-0.246B2O3-0.75PbO	12.77	1.7040	8.3	4.36	0.22	2.35	1.9516
	4	0.006 SeO2-0.244B2O3-0.75PbO	27.97	1.7022	10.17	5.36	0.21	2.29	1.7824
	5	0.002Cr2O3-0.248B2O3-0.75PbO	36.52	1.7893	13.1	5.95	0.213	3.46	1.7611
2nd series	6	0.004 Cr2O3-0.246B2O3-0.75PbO	67.38	1.6465	10.3	6.02	0.198	3.45	1.1970
	7	0.006 Cr2O3-0.244B2O3-0.75PbO	86.96	1.7603	17.23	8.21	0.20	3.49	1.4985
	8	0.002(SeO2+ Cr2O3)-0.248B2O3-0.75PbO	25.46	1.9330	14.26	5.43	0.23	1.79	1.8751
3rd series	9	0.004(SeO2+ Cr2O3)-0.246B2O3-0.75PbO	11.73	1.7408	8.71	4.29	022	2.36	1.9729
	10	0.006(SeO2+ Cr2O3)-0.244B2O3-0.75PbO	14.53	1.8329	10.76	4.56	0.23	1.8	1.6808

Three series of lead borate glasses of compositions $x$$Cr_2O_3$-(0.25-$x$)$B_2O_3$–0.75PbO,$x$$SeO_2$-(0.25-$x$)$B_2O_3$–0.75PbO and x(Cr_2O_3+SeO_2)-(0.25-x)B_2O_3–0.75PbO are prepared (Table 1), where x is the oxide molar fraction. The used raw materials were of chemically pure grade, in form of H_3BO_3, Cr_2O_3, SeO_2 and Pb_3O_4. The glass is prepared by melt quenching technique using porcelain crucibles in an electric furnace. The amount of the glass batch was 50 g $melt^{-1}$ and it was pre-heated at 500-600 ^oC, where the temperature of melting was 1100 °C. The duration of melting was one hour after the last traces of batches were disappeared. Then the melt was poured onto stainless steel mould and annealed at around 350^oC to remove thermal strains. Optical slabs were prepared by grinding and polishing of the prepared samples with paraffin oil and stannic oxide reaching minimum surface roughness tested by an interferometric method. Glass homogeneity was examined using two crossed polarizers.

2.2. Spectrophotometric Measurements

Computer aided two-beam spectrophotometer (shimadzu-3101PC UV-VIS NIR) was used to record the reflectance, R, and the transmittance, T, data of the plane-parallel slab glass samples, A resolution limit of 0.2 nm and a sampling interval of 2 nm were utilized for the different measuring points, The accuracy of measuring $R(\lambda)$, and $T(\lambda)$ is 0.003 with the incident beam making an angle of 5.0°± 0.1° to the normal to external slab faces. The 1240 measured points were carried out at room temperature for the entire spectral range 0.2-2.75 μm.

3. Theoretical Considerations

Nonlinear optics deals with strong electric field, E, that can alter the optical properties of materials to produce new fields altered in phase, frequency, and amplitude. The nonlinear polarization P of the material is given by [24]:

$$P = P_0 + \chi^{(1)}E + \chi^{(2)}EE + \chi^{(3)}EEE \quad (1)$$

where P_0 is the static dipole moment and $\chi^{(1)}$, $\chi^{(2)}$, and $\chi^{(3)}$are the first-, second-, and third-order susceptibilities, respectively. $\chi^{(1)}$ is acquainted for the linear optical properties, whereas $\chi^{(2)}$ is applied only to materials without inversion symmetry. Third-order susceptibility $\chi^{(3)}$ is considered for two-photon absorption (TPA), self-focusing and the quadratic Kerr effect.

In isotropic materials such as glasses the nonlinear response of interest for the glasses considered here is the second-order nonlinear refractive index n_2 which is given by:

$$\tilde{n} = n + n_2\langle E^2\rangle \quad (2)$$

where $\tilde{n}$ is the total refractive index, n is the linear one. When the optical frequency is below the electronic band gap, the self-focusing n_2 for laser beam in isotropic media can be attributed to electronic contribution which has a minimum response time of order of 10^{-16} s. It is faster than the time resolution provided by the shortest optical pulses available today (<10 fs). The electronic contribution of n_2 is of nonresonant type and it is included in the real part, Re$\chi^{(3)}$, of $\chi^{(3)}$, whereas the nonlinear absorption (or gain) contribution is of a resonant type and is included in the imaginary part, Im$\chi^{(3)}$, of $\chi^{(3)}$. Since the optical frequencies are too large as compared to the vibrational frequencies of the material, therefore, Re$\chi^{(3)}$ is large than Im$\chi^{(3)}$.

According to Miller's rule [25], the third-order susceptibility $\chi^{(3)}$ (as a complex quantity) of a material can be estimated by the linear refractive index value, n, using the following relation:

$$\chi^{(3)} = \left(\frac{n^2-1}{4\pi}\right)^4 \times 10^{-13} \text{ (esu)} \quad (3)$$

So, it means larger index of refraction induces larger $\chi^{(3)}$. According to Vogel et al. [26], $\chi^{(3)}$ as a function of second-order refractive index, n_2, is given by the relation:

$$n_2 = \chi^{(3)}(\times 10^{-13}\text{ esu})\frac{12\pi}{n} \quad (4)$$

Thus, a large index change may result in considerable nonlinear phase changes. The nonlinear directional coupler and optical bistability devices can be made on the basis of such optically induced phase changes.

Classification of optical nonlinearity into resonant- and nonresonant- nonlinear effects depends upon whether real or virtual states are involved in optical excitation. The nonresonant effect appears to have a better chance of success because of the minimal thermal dissipation that negatively affects the maximum data rate in optical telecommunication systems. The dispersion of the two parts $\chi^{(3)}$ (in esu) can be given by [27]:

$$\text{Re}\left|\chi^{(3)}\right| = 2\varepsilon_0 c n^2 n_2, \quad (5)$$

$$\text{Im}\left|\chi^{(3)}\right| = \frac{\varepsilon_0\, c\, n^2 \lambda}{2\pi}\beta \quad (6)$$

where c is speed of light, λ the wavelength, β is two-photon absorption coefficient (TPA), and ε_0 is the permittivity of vacuum. The TPA coefficient as a function of glass refractive index and the optical band gap energy, E_g, is given by [28, 29]:

$$\beta = KE_p^{1/2}F(2\hbar\omega/E_g)/n^2E_g^3 \quad (7)$$

The material-independent constant K is in cm/GW eV$^{5/2}$ and E_p is the Kane energy parameter. The material-independent spectral function $F(2\hbar\omega/E_g)$ as function of photon energy, $\hbar\omega$, is given by [30, 31]:

$$F(2\hbar\omega/E_g) = \frac{[(2\hbar\omega/E_g)-1]^{3/2}}{(2\hbar\omega/E_g)^5} \quad (8)$$

where $\hbar$ is Plank's constant and ω is the angular frequency. The photon energy range is selected at two wavelengths satisfying TPA condition where $E_g/2<\hbar\omega<E_g$.

Different attempts and empirical relations have been carried out to correlate nonlinear optical parameters such as n_2 (second-order nonlinear refractive index), β and $\chi^{(3)}$ to the linear refractive index and/or band gap energy [32-34]. Accordingly, Böling et al. [34] proposed a relation that connects n_2 to the linear refractive index and the glass Abbe number, V_d, where n_2 is given by:

$$n_2(10^{-13}\text{esu}) = 391\frac{(n-1)}{V_d^{5/4}} \quad (9)$$

The Abbe dispersion number is given by:

$$V_d = \frac{n_d-1}{n_F-n_C} \quad (10)$$

where n_F, n_d and n_C are the linear refractive indices at the following standard wavelengths: λ_F = 0.4613 μm, λ_d = 0.58756 μm and λ_C = 0.65627 μm. The calculated values of Abbe numbers are listed in Table 1.

At long wavelengths the value of the linear refractive index n_0 (static refractive index) can be related to structural dispersion parameters E_o and E_d by the following expression [35]:

$$n_0 = \sqrt{\frac{E_d}{E_0} + 1} \quad (11)$$

which obviously relates both the second-order index of refraction, n_2, and the third-order nonlinear optical susceptibility, $\chi^{(3)}$, to the structural and dispersion parameters of the investigated glasses. On the other hand, examining the refractive index data below the interband absorption edge found that normal dispersion of the energy dependence of refractive index satisfies a Sellmeier relation of the form [36]:

$$n^2 - 1 = \frac{E_0E_d}{E_0^2-E^2} \quad (12)$$

where E is the photon energy, E_o is the single oscillator energy (average oscillator energy for electrons), and E_d is the dispersion energy parameter of the material, all are in eV.

The parameter E_o is directly related to the optical band gap, whereas the parameter E_d is a measure of the strength of interband optical transitions. On other hand, E_d values are related to the nearest neighbor cation coordination, anion valency, ionicity, and effective number of dispersion electrons [36].

The dispersion parameters E_o and E_d are necessary to calculate a very important parameter for glasses which is the material dispersion $M(\lambda)$. This parameter determines the suitability of the glass to be used for optic fiber Telecom applications and it is defined by:

$$M(\lambda) = -\frac{\lambda}{c}\left(\frac{\partial^2 n}{\partial \lambda^2}\right) \quad (13)$$

Practically, $M(\lambda)$ is calculated in ps $nm^{-1}km^{-1}$ by the following expression [37]:

$$M(\lambda) = 1.54\times10^4 \frac{E_d/E_o^3}{n\lambda^3} - 2.17\times10^3 E_l^2 \frac{\lambda}{n} \quad (14)$$

where E_l is lattice energy in eV. The wavelength λ_{zero} (in μm) for zero material dispersion ($M = 0$) is calculated from Wemple's material three-parameter formula [37]:

$$\lambda_{zero} = 1.63\left(\frac{E_d}{E_o^3 E_l^2}\right)^{\frac{1}{4}} \quad (15)$$

4. Possible Structural Units of Lead Borate Base Glass

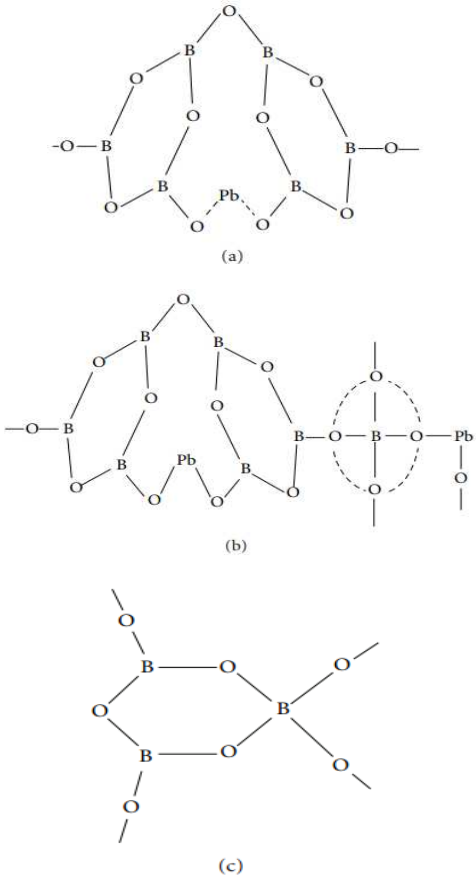

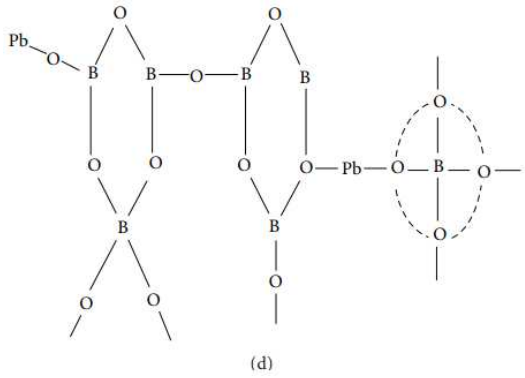

Fig 1. *(a) Possible structural units of PbO-B_2O_3 glasses, three coordinated boroxol rings modified by Pb^{2+}, (b): Formation of Pb–O–B covalent bands, (c): Bridge networks between [BO_3] and [BO_4] units and (d): Complex structures of Pb^{2+}-modified boron–oxygen rings and chains [38].*

The addition of 10–20 mol% PbO into the borate network does not affect its structure, where PbO acts as a network participant filled in the interspaces of [BO_3] units in the form of Pb^{2+} ions (Fig. 1(a)) [38]. The electrostatic fields of the strongly polarizing Pb^{2+} ions are affected with increase of PbO content. The addition of PbO leads to the conversion of [BO_3] units to [BO_4] units. Moreover, with increase of the content of PbO from 30 to 50 mol%, the formation of bridging bonds of Pb–O–B starts (Fig. 1(b)). Since the stretching force constant of Pb-O bonding is substantially lower than that of the B–O, the stretching frequency of Pb–O–B might tend to be lower. Another dominant, the presumption that B–O rings are formed in the glasses by the connection of the bridge oxygen ions between [BO_3] triangles and [BO_4] tetrahedrons can be made (Fig. 1(c)).

When the content of PbO increases up to 75 mol%, the content of Pb–O–B becomes dominant in the glass network structure. It can be presumed that, increasing polarization of Pb^{2+} with the increase of PbO content contributes to the formation of Pb^{2+}-modified boron–oxygen rings and their chains with also increasing the content of [BO_4] units. Subsequent additions of PbO (60–80 mol%) have the same effect on the structure of glasses. It can be concluded that, as PbO content exceeds 60 mol%; five bridging oxygens may be involved in glass networks: B–O–B in [BO_3] and [BO_4] units, the bridging oxygen ions between [BO_3] and [BO_4] units, Pb–O–B in bridge connection of [BO_3] and [BO_4] units, and Pb–O in covalent bonds (Fig. 1(d)). Addition of various oxide constituents, in PbO-B_2O_3 glasses, would affect also the structural properties of these glasses.

5. Results and Discussion

Fig. 2 elucidates the dispersion of the calculated refractive indices of the different prepared glass samples as a function of wavelength. The estimated error, δn, for the refractive index is 0·003. As shown in the figure, the refractive indices of the glasses in series 3 have higher relative values as equal share molar ratio of SeO_2 and Cr_2O_3 increases on the expense of B_2O_3. This behavior is attributed to increase in glass polarizability due to different factors arise from the

cooperation of negative sites with different binding energy including nonbridging oxygen bonds (NBOs) [39, 40]. The first factor is due to the BO_4^- units where negative charges are distributed around the boron atom (see Fig. 1(a) and 1(b)). The second factor is nonbridging oxygen atoms where the negative charge is localized on the B-O bond (see Fig. 1(c) and 1(d)) with deeper potential well. The third is a conversion of chromium ions from CrO_4^{2-} structural units to predominantly Cr^{3+} state in octahedral environment with nonbridging Cr–O^- bonds. Fourth, selenium oxide possesses selenate (SeO_4^{2-}) structure which acts as a modifier in the network with four coordinated oxygen and two lone pair of electrons. Thus the increase in these types of negative sites massively increases the glass polarizability.

According to electronic polarizability approach of the oxide ion through Fajans' rule [41], the polarization power (p) could be used to predict whether a chemical bond will be covalent or ionic. It depends on the charge Z on the cation and the ionic radius r of the cation in Å, where it is defined as $p = z/r^2$. Thus to increase the polarizability of the glass (i.e, increasing its refractive index) large Z and small r is required, so that the electronic shell of the oxygen ions is affected by the polarizing action of modifying ions leading to an increase in the concentration of NBOs. Therefore polarization power (field strength) increases due to the order B^{3+}> Se^{6+}> Cr^{3+}.Thus, it is predicted that the replacement of one B_2O_3 oxide by the co-participation of equal share of the two Cr_2O_3 and SeO_2 oxides will provide glass with more ionic behavior. This can describe the pronounced increase in refractive index that is in sample 8. It is clear that the dispersion measurements are very important when one is looking for nonlinear material characterization, especially if the incident wavelength of the pump beam is around the band gap energy, E_g, when the linear absorption cannot be neglected.

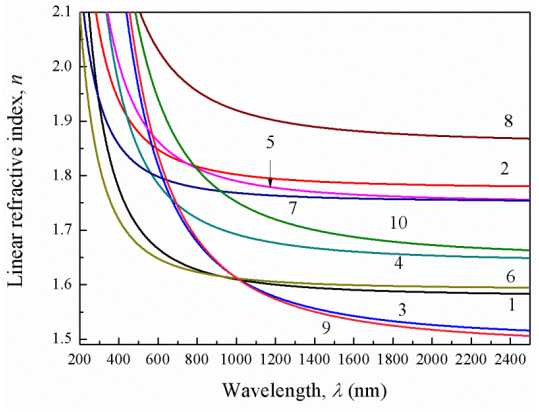

Fig 2. *Dispersion of the linear refractive index for all investigated glasses.*

5.1. Scaling of Oxide ion Polarizability with Refractive Index

On the basis of refraction data, Fig. 2, there is an intrinsic relationship exists between electronic polarizability of the oxide ions α_{O2-}, the local field inside the material and its refractive index n. Based on Lorentz- Lorenz equation, the refractive index based polarizability of oxide ions $\alpha_{O2-}(n)$ of oxide glasses can be determined by subtracting the cation polarizability from the molar polarizability [42, 43]:

$$\alpha_{O2-}(n) = [(V_m/2.52)(n^2-1)/(n^2 + 2)-\Sigma\alpha_i](N_{o2-})^{-1} \quad (16)$$

where V_m is molar volume, $\Sigma\alpha_i$ denotes molar cation polarizability and N_{o2-} denotes the number of oxide ions. For ternary glasses with a general formula $x_1A_pO_q$ $x_2B_rO_s$ $x_3C_nO_m$, where x denotes the molar fraction for each oxide, the oxide ion polarizability is calculated using the following equation denotes molar cation polarizability given by $x_1pa_A+x_2ra_B+x_3na_C$ and N_{O2-} denotes the number of oxide ions in the chemical formula given by $x_1q+x_2s+x_3m$. The molar volume of the present glass is taken from Ref. [40], while the molar cation polarizability $\alpha_{O2-}(n)$ of the glasses is calculated using the data on the polarizability of cations collected in Refs [44, 45]. The calculated polarizability values of oxide ions $\alpha_{O2-}(n)$ are plotted in Fig. 3 as a function of the refractive index n. It can be seen that there is a linear trend for increasing the oxide ion polarizability along with the increase in refractive index. Such line relation can be described by an empirical expression giving by:

$$\alpha_{O2-}(n)[Å^3] = 3.8\,n - 4.7 \quad (17)$$

The findings suggest that the refractive index of the glasses depend not only on the hydrostatic density but also on the polarizability of the glass. As Shown in Fig. 4, the values of oxide ions polarizabilities $\alpha_{O2-}(n)$ are plotted against oxide molar fraction, x, and from this figure it is clear that the third glass series which has a mixture of equal share of molar fractions of Cr_2O_3 and SeO_2 oxides will provide a glass with the higher oxide ions polarizability $\alpha_{O2-}(n)$, for example samples 8 and 10.

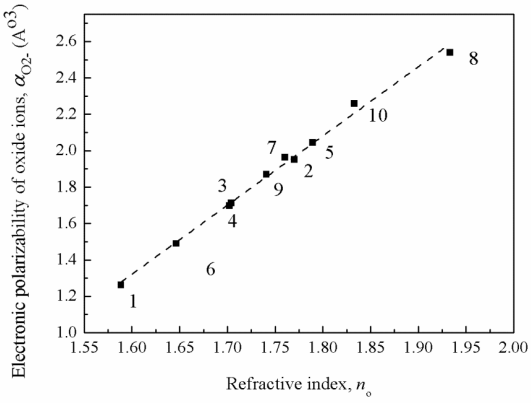

Fig 3. *The variation of calculated oxide ions polarizability $\alpha_{O2-}(n_o)$ plotted as a function of the refractive index, n.*

5.2. Scaling of Imaginary Part of Third-Order Susceptibility with Band Gap Energy

Ultrafast switching, signal regeneration, and high-speed demultiplexing that are used in high-capacity communication networks would be all-optically achieved through the design of third-order optical susceptibility. This

ultrafast response has been exploited in soliton propagation in glass fibers [46, 47], in the generation of femtosecond pulses in solid-state lasers [48] and in ultrafast all-optical-switching devices [49, 50].

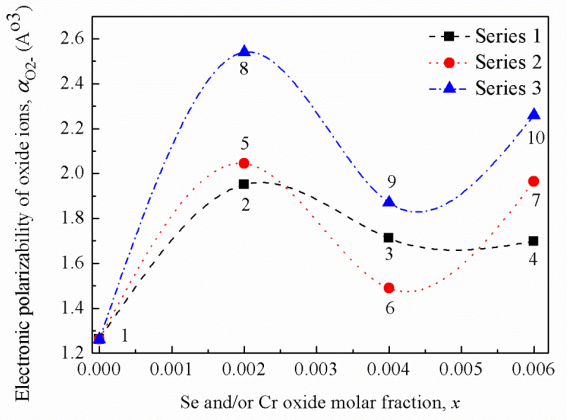

Fig 4. *Oxide ions polarizabilities $\alpha_{O2-}(n_o)$ versus substituted oxides molar fractions, x.*

Fig. 5 illustrates the calculated dispersion of real contribution of third-order susceptibilities, whereas Fig. 6 illustrates the effect of type of cation and its molar fraction on $Re\chi^{(3)}$. It is clear that the real susceptibility part follows the same trend of the glass linear refractive index indicating that the electronic polarizability is the origin of $Re\chi^{(3)}$.

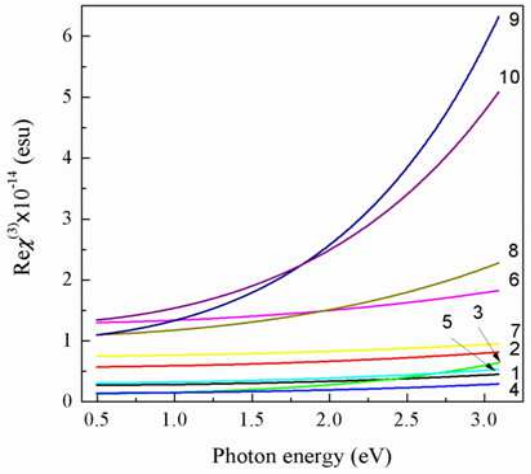

Fig 5. *The dispersion of real contribution of third-order susceptibilities.*

For comparison purpose between the different prepared glass samples $Re\chi^{(3)}$, Fig. 5, will be evaluated at λ_d = 587.56 nm. $Re\chi^{(3)}$ is varying from 3.4×10^{-15} esu (sample 1) to 6.7×10^{-15} esu as in case of 0.002 Cr_2O_3 mole fraction (sample 2). Also $Re\chi^{(3)}$ showed 15.2×10^{-15} esu with a 0.004 SeO_2 mole fraction (sample 6) while sample 9 with an equal share for molar fractions of Cr_2O_3 and SeO_2 provided 28.1×10^{-15} esu. At photon energy near to resonance frequency, sample 9 got $Re\chi^{(3)} = 63.3\times10^{-15}$ esu. Indeed the existence of the NBO's which are previously discussed [40] and their associated structural negative sites could not only explain such considerable value for $Re\chi^{(3)}$, specially that seen with glass sample 9.

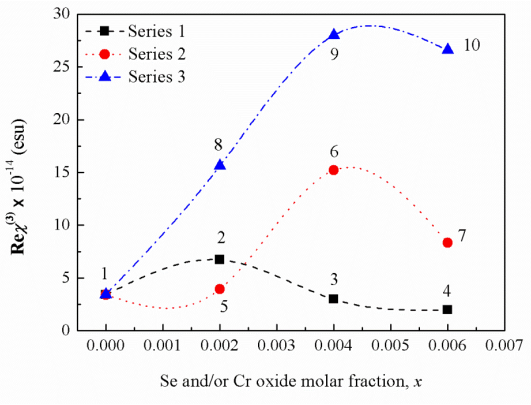

Fig 6. *Dependence of $Re\chi^{(3)}$ on the cation type and its oxide molar fraction.*

Quantum mechanical calculations demonstrate that bond hyperpolarizabilities generate the third-order susceptibility according to [24]:

$$\chi^{(3)} \cong \frac{N|\mu|^4}{\hbar^2(\omega_{0-}\omega)^2} \tag{18}$$

where N is the number density of optically active electrons if each atom possesses more than one outer-shell electron, μ is the resultant dipole transition moment, ω_0 is a characteristic resonance angular frequency and ω is the angular frequency of the incident light. Accordingly the resultant dipole transition moment of the glass, which is reinforced by an orbital hybridization [23, 51-54], governs the obtained third-order susceptibility.

Charge-transfer transitions of Se–O bonds may overlap with electronic transitions of Cr-O, resulting in significant changes in second-order bond hyperpolarizabilities. Due to valence *p* orbital of Se ion has a greater spatial extent than the *d* orbital of Cr ion, so the atomic orbitals that of *3d*-states of Cr atoms hybridize with that of *4p*-bands of Se atoms, and the *d–p* hybridized bands become broader [23, 40]. So by adjusting SeO_2 and Cr_2O_3 content levels and depending on the nature of valence orbitals, the substitution of *p*- and *d*-block elements results in lowering of conduction band. It leads to a drop in band gap to the semiconductor region [51-53] achieving the $Re\chi^{(3)}$ required for glass optoelectronic properties.

The dispersion of $Im\chi^{(3)}$ versus photon energy for different glass samples is shown in Fig. 7, while the effect of cation type and its molar fraction is shown in Fig. 8. Nonlinearity in glasses is reinforced by addition of either a second lone pair holder such as Se^{6+}, Pb^{2+} or cations with empty *d*-orbitals like Cr^{3+}.

Different reports [23, 55, 56] maintained that the electronegativity difference between the oxide cations and anions is responsible for the electronic structure of band gap of a material. Glasses with high-atomic-number anions and cations experience large optical polarizability resulting in small band gap and hence a large $Im\chi^{(3)}$ described by Eq. (6). It can be seen in Fig. 7 that, the dispersion of $Im\chi^{(3)}$ follows

the trend of two-photon absorption coefficient dispersion [23], that is described by Eq. (7). It indicates that sample 8 has also the highest $\mathrm{Im}\chi^{(3)}$ with maximum value of 4.97×10^{-12} m/GW.

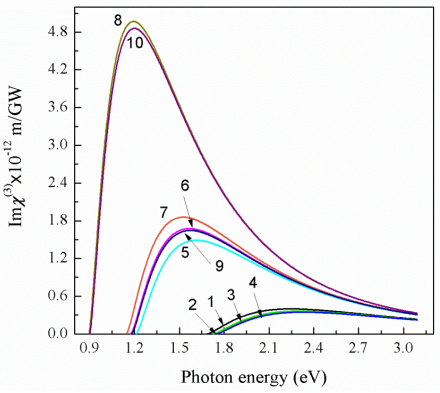

Fig 7. *Dispersion of the imaginary part contribution of $\chi^{(3)}$ for the investigated glass samples.*

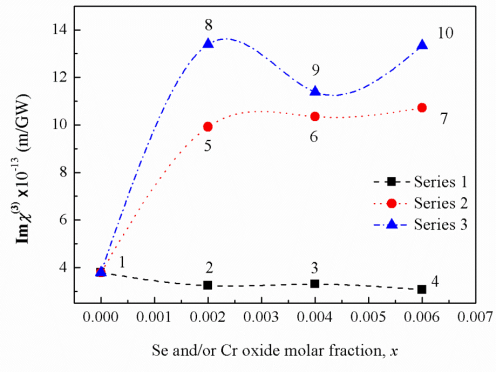

Fig 8. *Dependence of $\mathrm{Im}\chi^{(3)}$ on the cation type and its oxide molar fraction.*

At photon energies near the band gap energy, the dominant nonlinear optical mechanism is usually saturation of the exciton resonance of material. For photon energies greater than the band gap energy, the nonlinear response occurs as the result of excitation of electrons from valence band to conduction band. Resonant nonlinearities must involve the generation of carriers (electrons and holes). It leads to execute processes such as screening of the Coulomb potential, reduction of the band gap and filling of the conduction band, although modifications are possible by selection of network-modifying cations. According to Liu et al. [57], optical spectra in heavy metal oxide glass show typical features of electronic structure similar to those of crystalline semiconductors.

Van Stryland et al. [58] have proposed a simple but widely applicable model to predict TPA coefficient in semiconductors by using the parabolic band model, in their formulation, TPA coefficient β is in proportional to E_g^{-3}. In the same predisposition, Yuichi Watanabe [59] reported a $[E_g^{opt}]^{-1}$ proportionality for heavy metal glass, confirming the electronic structures base for β and hence $\mathrm{Im}\chi^{(3)}$. Furthermore, the variation in the nonlinear absorption coefficient, β, along with band gap energy, E_g, has been described by a universal linear relation for transition metal-containing oxide glasses [60].

For scaling purpose, a relation between $\mathrm{Im}\chi^{(3)}$ and direct optical energy gap E_g^d [23] (Table 1) at λ_d = 587.56 nm is carried out and is shown in Fig. 9. The variation could be described by an empirical linear expression given as:

$$\mathrm{Im}\,\chi^{(3)}\ (\times10^{-12}\ \mathrm{m/GW}) = 2.45 - 0.61\,E_g^d\ (\mathrm{eV}) \qquad (19)$$

Such proposed linear relation means that a drastic control of $\mathrm{Im}\chi^{(3)}$ by tailoring the optical band gap, i.e., the linear optical resonance could provide a way to tune the value of $\mathrm{Im}\chi^{(3)}$ by scheming the value of E_g. As shown in Fig. 10, the relation between the maximum value of $\mathrm{Im}\chi^{(3)}$ along with E_g is not linear any more, which is described the following expression:

$$\mathrm{Im}\chi^{(3)}_{max}\left(\times10^{-12}\,\frac{\mathrm{m}}{\mathrm{GW}}\right) = Ae^{-BE_g} + C \qquad (20)$$

where A, B and C are material-independent constants having the values of 207 ($\times10^{-12}$ m/GW), 2 $(\mathrm{eV})^{-1}$ and 0.2 ($\times10^{-12}$ m/GW), respectively. This gives possibility to calculate the so-called maximum $\mathrm{Im}\chi^{(3)}$ based on linear absorption using data of band gap energy of the glass.

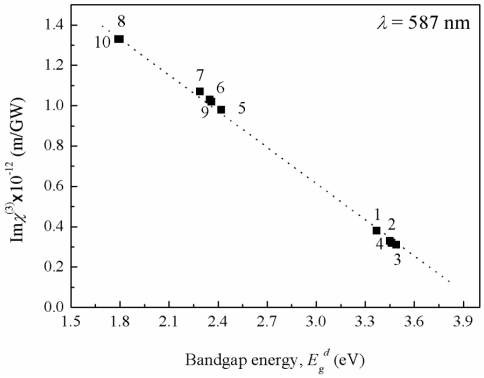

Fig 9. *Scaling the relation between $\mathrm{Im}\chi^{(3)}$ and E_g at λ_d = 587 nm.*

The astonishing observation is that when we divided the band gap energy over the photon energy at maximum $\mathrm{Im}\chi^{(3)}$ the ratio gives 1.5 for all glass samples. Such scaling ratio means that the value of photon energy correspondence to $\mathrm{Im}\chi^{(3)}_{max}$ can be determined once E_g is known.

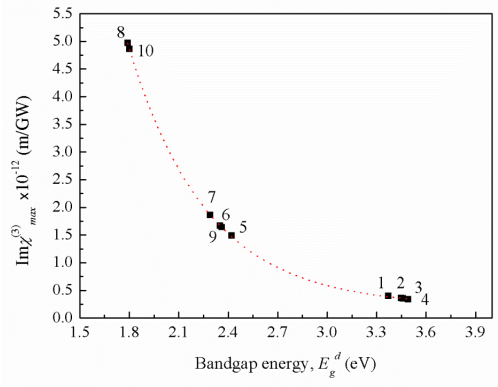

Fig 10. *The relation between the maximum value of $\mathrm{Im}\chi^{(3)}$ along with E_g.*

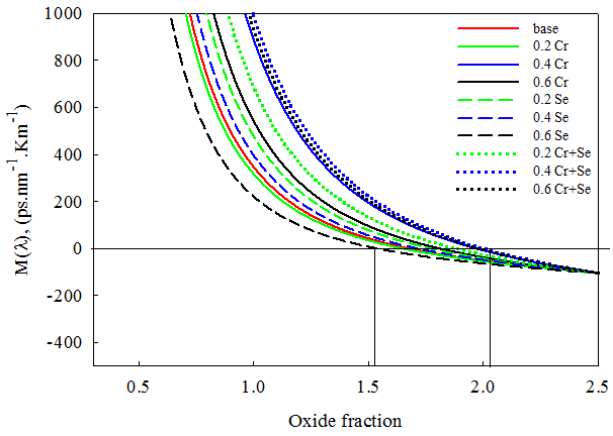

Fig 11. *Determination of obtained zero-dispersion wavelengths which are nearby 1.55 µm.*

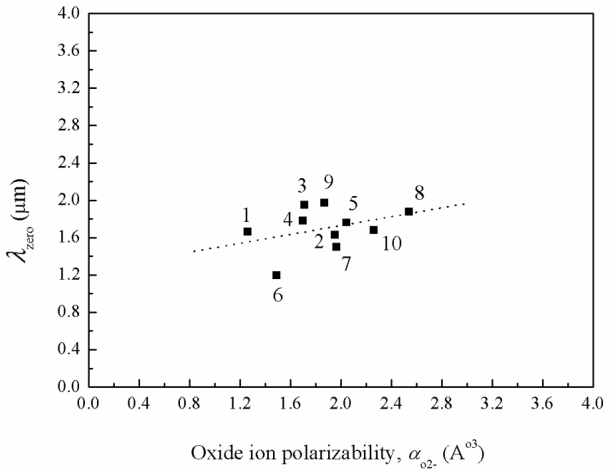

Fig 12. *Dependence of zero-dispersion wavelength, λ_{zero}, on the oxide electronic polarizability, α_{O2-}, for the studied glasses.*

Highly Nonlinear Fibers (HNLFs) made from heavy metal glasses [61] with tailored chromatic dispersion are of great interest for several photonic applications, ranging from supercontinuum generation to all-optical signal processing and optical parametric devices. Four-wave mixing (FWM) in fibers, due to glass transparency in terms of both modulation format and bit rate, is one of the most promising wavelength conversion mechanisms in high speed wavelength division multiplexed (WDM) optical networks. The effective nonlinear coefficient, γ, of a fiber is used in order to scale its performance for nonlinear device applications, which can be expressed as:

$$\gamma = \frac{2\pi n_2}{\lambda A_{eff}} \tag{21}$$

where A_{eff} is the effective mode area. On other hand, applications of supercontinuum generation involve a shifted chromatic dispersion profile, so that the zero-dispersion wavelength, λ_{zero}, of the nonlinear fiber is accurately positioned to match that of the pump light source. This can give rise to extreme spectral broadening even in a short fiber length [62].

The first promising result on the use of our prepared glass to be nonlinear dispersion-flattened optical fiber for operation around telecoms wavelength 1.55 µm is its high nonlinearity. In order to achieve dispersion minimized propagation it is desirable that the material of the optical waveguide should have nearly zero group velocity dispersion (GVD) at the operating wavelength for communication. Generally 1.55 µm is used in majority cases of communication network. For fused silica GVD is zero at 1.27 µm. Wavelength for zero dispersion is also an essential parameter needed for different application such as fiber optical parametric amplifiers, parametric gain and wavelength conversion, parametric oscillator, parametric soliton laser, and ultrafast all optical switching [63-67].

Consequently, the second encouraging result is indeed the obtained zero-dispersion wavelengths according to Eq. (14), as shown in Fig. 11 and Table 1. Samples 1, 2, 7 and 10 exhibit zero group velocity dispersion with zero-dispersion wavelengths nearby 1.55 µm. As shown in Fig. 12, the zero-dispersion wavelength increases with increasing the glass electronic polarizability. Therefore we can confirm, as it was previously concluded [68], that controlling the glass electronic polarizability is one of the ways to tailoring the wavelength for zero dispersion at the Telecom operating wavelengths. For instance, the wavelength for zero material dispersion is proportional to the parameter E_d which is a measure to the strength of interband optical transitions.

It is found that E_d obeys a simple empirical relationship [36] $E_d = \kappa N_c Z_a N_e$, where N_c is the coordination number of the cation nearest neighbor to the anion, Z_a, is the formal chemical valency of the anion, N_e, is the effective number of valence electrons per anion (usually N_e = 8), and κ is essentially two-valued, taking on the "ionic" value κ = 0.26 + 0.04 eV for halides and most oxides, and the "covalent" value κ = 0.37 + 0.05 eV for the tetrahedral bond type structures [36]. The calculated values of E_d, E_0 and E_l for the investigated glass samples are listed in Table 1. It is suggested that the dependence of E_d on coordination number and valency implies that an understanding of wavelength for zero dispersion behavior may lie in a localized molecular theory of optical transitions and molecular orbital hybridization.

Orbital hybridization between the different integrated oxides affects the glass physical properties reaching to optimize the glass functions and its processing parameters. Combination of structural and optical properties is achievable as a result of structural variability in glasses since more than one structural unit may exist. SeO_2 exists as one dimensional polymeric chain with alternating selenium and oxygen atoms. Cr_2O_3 consists of a hexagonal close packed array of oxide anions with 2/3 of the octahedral holes occupied by chromium.

PbO occurs in two polymorphs, one having a tetragonal crystal structure and the other having an orthorhombic crystal structure. B_2O_3 is composed of structural groupings as boroxol, tetraborate, diborate, microdomains of boroxol rings making BO_3 triangles depend on composition and on preparation conditions. The presence of multiple structural

moieties creates a range of dipole environment which is ideal for tailoring the glass electronic structure and hence its optical and photonic applications.

6. Conclusion

We have determined the frequency dependence of the nonlinear optical susceptibilities of heavy metal borate glass to demonstrate the relative contributions of both "electronic polarization" and "hybridization" mechanisms to the glass nonlinearity. It is found that $\chi^{(3)}$ increases as the ionic radius of both network modifiers and intermediates decreases. Glasses with high-atomic-number cations and large field strength experience large optical polarizability resulting by large orbital hybridization. Substitution of SeO_2 by B_2O_3 makes the base glass to have a more pronounced semiconducting character while Cr_2O_3 caused the base material to have an insulating property. However, the substitution of SeO_2 and/or Cr_2O_3+SeO_2 by B_2O_3 derives the glass to have semiconducting-like features. The rise in nonlinear index is then governed by the nonlinear bond polarizabilities of the Se–O and Cr-O bonds. Charge-transfer transitions of Se–O bonds overlap with electronic transitions of Cr-O, resulting only in considerable changes in bond hyperpolarizabilities. Scaling of oxide ion polarizability with refractive index and scaling of imaginary part of third-order susceptibility with band gap energy are proposed. The material dispersion obtained from refractive index measurements exhibit a glass with zero-dispersion wavelengths fall in the 1.55 μm Telecom propagation band.

Acknowledgement

The work is supported by the National Research Centre, Dokki, Egypt project no. 10070402.

References

[1] F. El-Diasty, F. A. Abdel Wahab, and M. Abdel-Baki, “Optical band gap studies on lithium aluminum silicate glasses doped with Cr^{3+} ions,” J. Appl. Phys. 100 (2006) 093511-17.

[2] G. L. Flower, M. S. Reddy, G. S. Baskaran, and N. Veeraiah, "The structural influence of chromium ions in lead gallium phosphate glasses by means of spectroscopic studies," Opt. Mater.30 (2007) 357-363.

[3] V. Petricevic, S. K. Gayen, and R. R. Alfano, "Laser action in chromium-activated forsterite for near-infrared excitation: Is Cr^{4+} the lasing ion?" Appl. Phys. Lett. 53 (1988) 2590-2592.

[4] G. Tang, Z. Yang, L. Luo, and W. Chen, "Dy^{3+}-doped chalcohalide glass for 1.3 μm optical fiber amplifiers," J. Mater. Res. 23 (2008) 954–961.

[5] G. Tang, H. Xiong, W. Chen, and L. Luo, "The study of Sm^{3+}-doped low-phonon-energy chalcohalide glasses," J. Non-Cryst. Solids 357 (2011) 2463–2467.

[6] J. A. Savage, "Optical-Properties of Chalcogenide Glasses," J. Non-Cryst Solids 47 (1982) 101-116.

[7] A. B. Seddon, "Chalcogenide Glasses - a Review of Their Preparation, Properties and Applications," J. Non-Cryst Solids 184 (1995) 44-50.

[8] V. G. Ta’eed, N. J. Baker, L. Fu, K. Finsterbusch, M. R.E. Lamont, D. J. Moss, H. C. Nguyen, B. J. Eggleton, D. Y. Choi, S. Madden, and B. Luther-Davies, "Ultrafast all-optical chalcogenide glass photonic circuits," Opt. Express 15 (2007) 9205-9221.

[9] M. Abdel-Baki, and F. El-Diasty, "Glasses for photonic technologies," Int. J. Opt. Appl. 3 (2013) 125-137.

[10] A. Zakery, and S.R. Elliott, "Optical Nonlinearities in Chalcogenide Glasses and Their Applications," Springer 2007.

[11] R. E. Youngman, and J. W. Zwanziger, "Multiple boron sites in borate glass detected with dynamic angle spinning nuclear magnetic resonance," J. Non-Crystal. Solids 168 (1994) 293-297.

[12] P. Becker, "Borate Materials in Nonlinear Optics," Adv. Mater. 10 (1998) 979-992.

[13] N. M. Bobkova, and S. A. Khot’ko, "Structure of zinc-borate low-melting glasses derived from IR spectroscopy data," J. Appl. Spectro. 72 (2005) 853-857.

[14] C. B. Layne W. H. Lowdermilk, and M. J. Weber, “Multiphonon relaxation of rare earth ions in oxide glasses”, Phys. Rev. B 16 (1977) 10-20.

[15] Z. Burshtein, “Radiative, nonradiative, and mixed-decay transitions of rare-earth ions in dielectric media”, Opt. Eng. 49 (2010) 091005.

[16] Z. L. Wang, and Z. C. Kang, "Functional and Smart Materials — Structural Evolution and Structure Analysis," New York: Plenum Press, 1998.

[17] S. Şimşek, "A novel method for designing one dimensional photonic crystals with given bandgap characteristics," AEU – Inter. J. Electron. Commun. 67 (2013) 827-832.

[18] F. El-Diasty, “Theoretical and experimental evaluation of the modal field-shift and the associated transition loss in perturbed index-profile single-mode optical fiber applying Fizeau interferometry,” J. Opt. Soc. Am. A 21 (2004) 1496-1502.

[19] F. El-Diasty, “Evaluation of some GRIN fiber parameters and associated fraction mode loss due to mechanically induced optical anisotropy,” Appl. Opt. 42 (2003) 5263-5273.

[20] F. El-Diasty, A. Amichi, “Evanescent-wave in perturbed optical fibers,” Opt. Commun. 281 (2008) 4329-4333.

[21] F. El-Diasty, H. A. El-Hennawi, “Nonlinearity in bent optical fibers,” Appl. Opt. 48 (2009) 3818-3822.

[22] D. H. Heiman, R. W. Hellwarth, D. S. Hamilton, "Raman scattering and nonlinear refractive index measurements of optical glasses," J. Non-Cryst. Solids 34 (1979) 63-79.

[23] F. El-Diasty, F. A. Moustafa, F. A. Abdel-Wahab, M. Abdel-Baki, and A. M. Fayad, "Role of 4*p*-3*d* orbital hybridization on band gap engineering of heavy metal glass for optoelectronic applications" J. Alloy. Comp. 605 (2014) 157-163.

[24] R. W. Boyd, Nonlinear Optics, 2nd ed. (Academic, 2003).

[25] R. C. Miller, “Optical second harmonic generation in piezoelectric crystals,” Appl. Phys. Lett. 5 (1964) 17–19.

[26] E. M. Vogel, M. J. Weber, and D. M. Krol, "Nonlinear optical phenomena in glass," Phys. Chem. Glasses 32 (1991) 231-254.

[27] T. Cassano, R. Tommasi, M. Ferrara, F. Babudri, G. M. Farimol, and F. Naso, “Substituent-dependence of the optical nonlinearities in poly(2,5-dialkoxy-p-phenylenevinylene) polymers investigated by the Z-scan technique,” Chem. Phys. 272 (2001) 111–118.

[28] M. Sheik-Bahae, D. J. Hagan, and E. W. Van Stryland, “Dispersion and band-gap scaling of the electronic Kerr effect in solids associated with two-photon absorption,” Phys. Rev. Lett. 65 (1990) 96–99.

[29] M. Sheik-Bahae, and E. W. Van Stryland, in: E. Garmire, A. Kost, eds., Semiconductors and Semimetals (Academic, 1999), Vol. 58, Chap. 4.

[30] M. Weiler, “Nonparabolicity and exciton effects in two-photon absorption in zincblende semiconductors,” Solid State Commun. 39 (1981) 937–940.

[31] B. S. Wherrett, “Scaling rules for multiphoton interband absorption in semiconductors,” J. Opt. Soc. Am. B 1 (1984) 67–72.

[32] V. Dimitrov, and S. Sakka, “Linear and nonlinear optical properties of simple oxides. II,” J. Appl. Phys. 79 (1996) 1741–1745.

[33] H. Ticha´, and L. Tichy´, “Semiempirical relation between nonlinear susceptibility (refractive index), linear refractive index and optical gap and its application to amorphous chalcogenides,” J. Optoelectron. Adv. Mater. 4 (2002) 381–386.

[34] N. L. Böling, A. J. Glass, and A. Owyoung, “Empirical relationships for predicting nonlinear refractive index changes in optical solids,” IEEE J. Quantum Electron. 14 (1978) 601–608.

[35] K. Petkov, and P. J. S. Ewen, "Photoinduced changes in the linear and non-linear optical properties of chalcogenide glasses," J. Non-Cryst. Solids 249 (1999) 150-159.

[36] S. H. Wemple, and M. DiDomenico, "Behavior of the electronic dielectric constant in covalent and ionic materials," Phys. Rev. B 3 (1971) 1338-1351.

[37] S. H. Wemple, "Material dispersion in optical fibers," Appl. Opt. 18 (1979) 31-35.

[38] C. Gautam, A. K. Yadav, and A. K. Singh, "A Review on infrared spectroscopy of borate glasses with effects of different additives," ISRN Ceramics 2012 (2012) 1-17.

[39] M. Abdel-Baki, F. A. Abdel Wahab, A. Radi, and F. El-Diasty, “Factors affecting optical dispersion in borate glass systems,” J. Phys. Chem. Solids 68 (2007) 1457-1470.

[40] F. A. Moustafa, M. Abdel-Baki, A. M. Fayad**,** and F. El-Diasty, "Role of mixed valence effect and orbital hybridization on molar volume of heavy metal glass for ionic conduction pathways augmentation," Am. J. Mater. Sci. 4 (2014) 119-126.

[41] K. Fajans, "Struktur und deformation der elektronenhüllen in ihrer bedeutung für die chemischen und optischen eigenschaften anorganischer verbindungen". *Naturwiss.* 11 (1923) 165–72.

[42] V. Dimitrov, and S. Sakka, "Electronic oxide polarizability and optical basicity of simple oxides," J. Appl. Phys. 79 (1996) 1736-1740.

[43] V. Dimitrov, and T. Komatsu, "Classification of oxide glasses: a polarizability approach," J. Solid State Chem. 178 (2005) 831-846.

[44] J. R. Tessman, A. H. Kahn, and W. Shockley, "Electronic Polarizabilities of Ions in Crystals," Phys. Rev. 92 (1953) 890-895.

[45] V. Dimitrov, and T. Komatsu, "An interpretation of optical properties of oxides and oxide glasses in terms of the electronic ion polarizability and average single bond strength," J. Univ. Chem. Tech. Metallurgy, 45 (2010) 219-250.

[46] L. F. Mollenauer, R. H. Stolen, and J. P. Gordon, "Experimental observation of picosecond pulse narrowing and solitons in optical fibers," Phys. Rev. Lett. 45 (1980) 1095-1097.

[47] G. P. Agrawal, *Nonlinear fiber optics*, 2nd ed. San Diego: Academic Press, 1995.

[48] D. E. Spence, P. N. Kean, and W. Sibbett, "60-Fsec pulse generation from a self-mode-locked Ti-sapphire laser," Opt. Lett. 16 (1991) 42-44.

[49] H. M. Gibbs, Optical Bistability: Controlling Light with Light," Orlando: Academic Press, 1985.

[50] M. N. Islam, *"Ultrafast Fiber Switching Devices and Systems*," Cambridge England; New York, NY, USA: Cambridge University Press, 1992.

[51] U. Häussermann, M. Boström, P. Viklund, Ö. Rapp, and T. Björnängen, "$FeGa_3$ and $RuGa_3$: Semiconducting Intermetallic Compounds," J. Solid State Chem. 165 (2002) 94–99.

[52] S. T. Lim, T. W. Kim, S. G. Hur, S.-Ju Hwang, H. Park, W. Choi, and J.-Ho Choy," Effects of p- and d-block metal co-substitution on the electronic structure and physicochemical properties of $InMO_4$ (M = Nb and Ta) semiconductors," Chem. Phys. Lett. 434 (2007) 251–255.

[53] M. Kobayashi, Y. Ishida, J. I. Hwang, G. S. Song, M. Takizawa, A. Fujimori, Y. Takeda, T. Ohkochi, T. Okane, Y. Saitoh, H. Yamagami, Amita Gupta, H. T. Cao, and K. V. Rao, "Hybridization between the conduction band and 3*d* orbitals in the oxide-based diluted magnetic semiconductor $In_{2-x}V_xO_3$," Phys. Rev. B 79 (2009) 205-203.

[54] S. Kundua, N. Das, S. Chakrabortya, D. Bhattacharya, and P. K. Biswas, "Synthesis of sol–gel based nanostructured Cr(III)-doped indium tin oxide films on glass and their optical and magnetic characterizations," Opt. Mater. 35 (2013) 1029–1034.

[55] J. B. Goodenough, "Descriptions of outer d electrons in thiospinels," J. Phys. Chem. Solids 30 (1969) 261–280.

[56] M. Abdel-Baki, Fathy A. Abdel-Wahab, and Fouad El-Diasty, "One-photon band gap engineering of borate glass doped with ZnO for photonics applications," J. Appl. Phys. 111 (2012) 073506.

[57] X. Liu, D. B. Hollis, and J. McDougall, "Ultraviolet absorption edge studies of heavy metal oxide glasses," Phys. Chem. Glasses 37 (1996) 160-168.

[58] E. W. van Stryland, M. A. Woodall, H. Vanherzeele, and M. J. Soileau, "Energy band-gap dependence of two-photon absorption," Opt. Lett. 10 (1985) 490-492.

[59] Y. Watanabe, S. Sakata, T. Watanabe, and T. Tsuchiya, "Two-photon absorption in binary Bi_2O_3-B_2O_3 glass at 532 nm," Journal of Non-Crystalline Solids 240 (1998) 212-220.

[60] F. El-Diasty, and M. Abdel-Baki, "One- and two-photon absorption in transition metal oxide glasses," J. Appl. Phys. 106 (2009) 053521.

[61] X. Feng, F. Poletti, A. Camerlingo, F. Parmigiani, P. Petropoulos, P. Horak, G. M. Ponzo, M. Petrovich, J. Shi, W. H. Loh, and D. J. Richardson, "Dispersion controlled highly nonlinear fibers for all-optical processing at telecoms wavelengths," Opt. Fiber Technol. 16 (2010) 378–391.

[62] J. M. Dudley, and J.R. Taylor (Eds.), Supercontinuum Generation in Optical Fibers, Cambridge University Press, 2010.

[63] M. E. Marhic, N. Kagi, T. -K. Chiang, and L. G. Kazovsky, "Broadband fiber optical parametric amplifiers," 21 Opt. Lett. (1996) 573-575.

[64] M. R. E. Lamont, C. M. de Sterke, and B. J. Eggleton, "Dispersion engineering of highly nonlinear As_2S_3 waveguides for parametric gain and wavelength conversion," Opt. Exp. 15 (2007) 9458-9463.

[65] G. K. L. Wong, S. G. Murdoch, R. Leonhardt, J. D. Harvey, and V. Marie, "High conversion-efficiency widely-tunable all fiber optical parametric oscillator," Opt. Exp. 15 (2007) 2947-2952.

[66] K. Suzuki, M. Nakazawa, and H. A. Haus, "Parametric soliton laser," Opt. Lett. 15 (1989) 320-322.

[67] N. Nishizawa, and T. Goto "Ultrafast all optical switching by use of pulse trapping across zero-dispersion wavelength," Opt. Exp. 11 (2003) 359-365.

[68] S. Fujino, and K. Morinaga, "Material dispersion and its compositional parameter of oxide glasses," J. Non-Cryst. Solids 222 (1997) 316-320.